NON-COPLANAR CRACK GROWTH

S. Nemat-Nasser
Northwestern University, Evanston, Ill. 60201, USA

Some recent analytical results on branched-curved extension of a pre-existing straight crack in brittle solids are reviewed, considering both overall tensile and overall compressive stress fields. Experimental observations are mentioned, and certain common failure mechanisms which stem from unstable non-coplanar crack extension are briefly discussed. Under overall compression, these include axial splitting, sheet fracture, rock-burst, and surface spalling.

INTRODUCTION

Material heterogeneity, the nature of applied loads, and other factors often cause non-coplanar extension of pre-existing straight cracks in brittle solids. Figures 1 to 4 illustrate this fact. In Fig. 1, the pre-existing straight edge cracks, AB, A_1B_1, and A_2B_2, in a glass plate are made to grow by the application of a concentrated heat source at points A, A_1, and A_2. The central crack grows co-linearly, whereas the other two cracks curve toward the free edges of the glass plate. Crack A_2B_2 is not at a right angle with respect to the free edge, AA_2, of the plate. Upon the application of a concentrated heat source at points A and A_2, the pre-existing crack AB smoothly curves toward the closest free glass edge with almost no initial "kink," whereas A_2B_2 extends with a sharp initial kink, followed by a smooth curve. Figures 2 and 3 illustrate "kinked-curved" crack growth under overall compressive far-field loads. Upon the application of axial compression, the pre-existing crack AB in Fig. 2 kinks away at an angle of about 70° from its initial path, curving toward a direction parallel to the applied compressive force. Figure 3, on the other hand, shows crack initiation (and growth) from the edges of a hard inclusion (aluminium) embedded in a soft (Columbia Resin CR39) plate, subjected to overall axial compression. In this case, a "microcrack" first develops along the interface between the hard inclusion and the matrix, and then crack growth occurs with a sharp initial kink followed by a smooth continuous curve; see Fig. 4. At Northwestern University, the author and co-workers have made many other experiments which show that non-coplanar crack extension is a rather common failure mode in brittle solids; see, for example, Karihaloo and Nemat-Nasser [1] and Nemat-Nasser and Horii [2]. Other

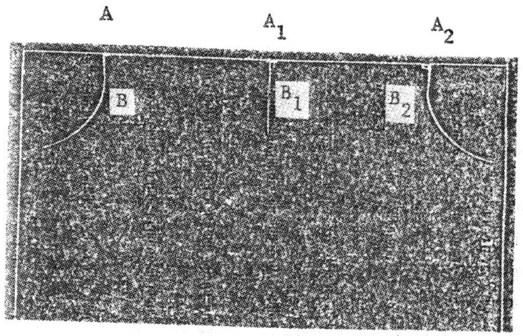

Figure 1

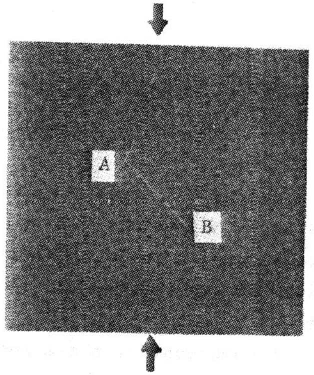

Figure 2

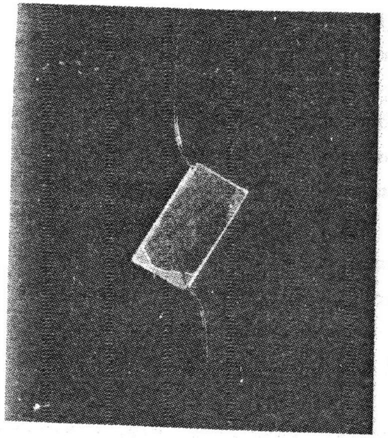

Figure 3

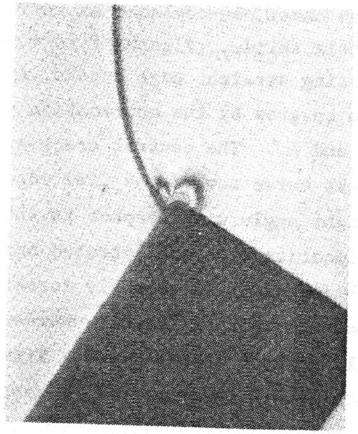

Figure 4

earlier experiments on crack growth in compression are, for example, Brace and Bombolakis [3], Bieniawski [4], Hoek and Bieniawski [5], Fairhurst and Cook [6], Ingraffea [7], and Holzhausen [8].

The analysis of crack branching under overall tension has been considered by a number of authors; see, for example, Andersson [9], Banichuk [10], Hussain, Pu and Underwood [11], Goldstein and Salganik [12], Bilby, Cardew and Howard [13], Kitagawa and Yuuki [14], Palaniswamy and Knauss [15], Wu [16-18], Lo [19], Cotterell and Rice [20], Karihaloo, Keer and Nemat-Nasser [21], Karihaloo, Keer, Nemat-Nasser and Oranratnachai [22],

Nemat-Nasser [23,24], Hayashi and Nemat-Nasser [25-27], and Karihaloo [28] who presents an overview of the basic recent results in this field. Palaniswamy and Knauss [15] and Lo [19] also discuss some of the existing literature. Branched-curved crack growth under overall compression, on the other hand, has not received much attention. References to some existing work are given by Holzhausen [8] and Nemat-Nasser and Horii [2].

For small kink angles and for slight deviations from straightness, perturbation methods have been used to estimate the initial paths of tension non-coplanar cracks [10,20,22], as well as those of compression-induced ones [2]. For large deviations, on the other hand, complete analytic formulations and results are given by Lo [19] for tension cracks, and by Nemat-Nasser and Horii [2] for frictional compression cracks.

In this paper, some existing analytical results for branched-curved crack growth are discussed, emphasizing the cases when under far-field compressive loads the pre-existing cracks undergo frictional sliding which produces kinked-curved tension cracks that may lead to overall anisotropic failure modes. Rock splitting, rockburst in deep mines, exfoliation, and surface spalling are examples of this type of failure.

FORMULATION

Attention is focused on plane problems (plane strain or plane stress). Muskhelishvili's [29] complex potentials are used. First these potentials are obtained for a single dislocation close to a pre-existing crack across which certain conditions are satisfied, and then with these potentials as the basic Green's functions, curved crack extension is formulated by distributing suitable dislocations along the crack path in such a manner that stress-free conditions are attained there. The integrals thus extend over the extended crack path only (rather than over the pre-existing crack and its extension), resulting in considerable reduction in numerical efforts.

Figure 5 shows a pre-existing crack, AB, and a single dislocation α at point $z_0 = x_0 + iy_0$, $i = \sqrt{-1}$. In terms of the analytic functions Φ and Ψ, the stress and displacement components are

$$\sigma_x + \sigma_y = 2(\Phi' + \overline{\Phi'}), \quad \sigma_y - \sigma_x + 2i\tau_{xy} = 2(\bar{z}\Phi'' + \Psi'),$$
$$2G(u_x + iu_y) = \kappa\Phi - z\overline{\Phi'} - \bar{\Psi}, \tag{1}$$

where G is the shear modulus, $\kappa = 3 - 4\nu$ for plane strain, $\kappa = \frac{3-\nu}{1+\nu}$ for plane stress, ν is Poisson's ratio, prime denotes derivative, superposed bar denotes the complex conjugate, and subscripts x and y represent

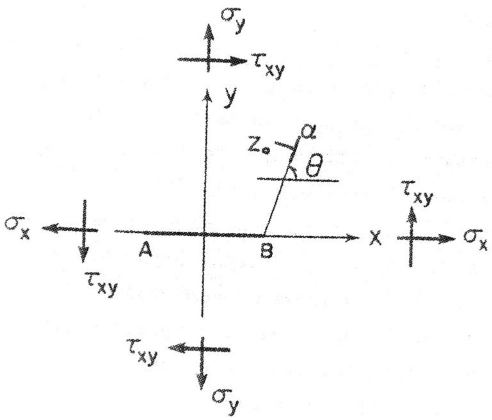

Figure 5

the corresponding rectangular Cartesian x and y components.

In the absence of any cracks (a homogeneous plate), the stress field produced by the dislocation

$$\alpha = Gbe^{i\theta}/i\pi(\kappa+1),$$
$$b = [u_r] + i[u_\theta], \qquad (2)$$
$$[u_r] = u_r^+ - u_r^-,\ [u_\theta] = u_\theta^+ - u_\theta^-,$$

is solved by the following stress functions:

$$\Phi_0 = \alpha\ \ell n(z - z_0),$$
$$\Psi_0 = \bar{\alpha}\ \ell n(z - z_0) - \alpha\ \bar{z}_0/(z - z_0). \qquad (3)$$

The normal and shear tractions introduced on the x-axis by these potentials are given by

$$p^0(x,z_0) \equiv \sigma_y^0 - i\tau_{xy}^0 = \alpha[\hat{f}(x,z_0) + \hat{f}(x,\bar{z}_0)] + \bar{\alpha}(z_0 - \bar{z}_0)\hat{g}(x,\bar{z}_0), \qquad (4)$$

where

$$\hat{f}(z,z_0) = (z - z_0)^{-1}, \quad \hat{g}(z,z_0) = (z - z_0)^{-2}. \qquad (5)$$

1. An Open Pre-existing Crack

When the overall far-field conditions are such that the pre-existing crack remains open during the branched-curved crack growth, then additional potentials, Φ_R and Ψ_R, are introduced in order to satisfy

$$\sigma_y - i\tau_{xy} = 0 \quad \text{for } y = 0 \text{ and } |x| < c. \qquad (6)$$

These stress potentials are obtained in such a manner that they correspond to tractions $-p^0(x,z_0)$ on $y = 0$ and $|x| < c$; Eq. (4). Following Muskhelishvili [29], Erdogan [30], Rice [31], and others, a Hilbert problem is solved with $-p^0(x,z_0)$ prescribed on the pre-existing crack. This corresponds to

$$\Phi_R' = \frac{-1}{2\pi i X(z)} \int_{-c}^{c} \frac{X(x)p^0(x,z_0)dx}{x - z} + \frac{C}{X(z)}, \quad X(z) = (z^2 - c^2)^{\frac{1}{2}}, \qquad (7)$$

where C is fixed such that a single-valued displacement field results. Since

$$\frac{1}{2\pi i X(z)} \int_{-c}^{c} \frac{X(x)}{x - z}\hat{f}(x,\pm z_0)dx = \frac{1}{2}\Big[1 \mp \Big(\frac{z_0^2 - c^2}{z^2 - c^2}\Big)^{\frac{1}{2}}\Big]\frac{1}{z \mp z_0} - \frac{1}{2}\frac{1}{(z^2 - c^2)^{\frac{1}{2}}}, \qquad (8)$$

it follows that $C = -\alpha$, and

$$\Phi_R'(z) = -\alpha[\hat{F}(z,z_0) + \hat{F}(z,\bar{z}_0)] - \bar{\alpha}(z_0 - \bar{z}_0)\hat{G}(z,\bar{z}_0),$$
$$\Psi_R'(z) = \bar{\Phi}_R'(z) - \Phi_R'(z) - z\Phi_R'', \qquad (9)$$

where

$$\hat{F}(z,z_0) = \frac{1}{2}\Big[1 - \frac{X(z_0)}{X(z)}\Big]\frac{1}{(z - z_0)} \quad \text{and} \quad \hat{G}(z,z_0) = \frac{\partial}{\partial z_0}\hat{F}(z,z_0). \qquad (10)$$

This result has been given by Lo [19].

2. A Closed Frictional Pre-existing Crack

It is assumed that a cohesive force, τ_c, acts across the closed crack which also transmits frictional forces. The shear stress (assumed negative) across the crack then is

$$\tau_{xy}^+ = \tau_{xy}^- = -\tau_c + \mu\sigma_y \quad \text{for } y = 0 \text{ and } |x| < c, \qquad (11)$$

where $\sigma_y < 0$ is assumed, and μ is the coefficient of friction. The additional stress potentials, Φ_R and Ψ_R, are then obtained in such a manner that

$$p(x,z_0) \equiv \sigma_{yR} - i\tau_{xyR} = i\tau_{xy}^0 - i\mu\sigma_y^0$$
$$= (\bar{\alpha}\bar{\beta} - \alpha\beta)[\hat{f}(x,z_0) + \hat{f}(x,\bar{z}_0)] + (\bar{z}_0 - z_0)[\bar{\alpha}\beta\hat{g}(x,\bar{z}_0) + \alpha\bar{\beta}\hat{g}(x,z_0)] \qquad (12)$$

is attained on $y = 0$, $|x| < c$, where $\beta = \frac{1}{2}(1 + i\mu)$; note $\sigma_{yR} = 0$. The final solution hence is, using (7) and (8),

$$\Phi_R'(z) = (\bar{\alpha}\bar{\beta} - \alpha\beta)[\hat{F}(z,z_0) + \hat{F}(z,\bar{z}_0)] + (\bar{z}_0 - z_0)[\alpha\bar{\beta}\hat{G}(z,z_0) + \bar{\alpha}\beta\hat{G}(z,\bar{z}_0)], \qquad (13)$$

where $C = (\bar{\alpha}\bar{\beta} - \alpha\beta)$, and $\hat{F}(z,z_0)$ and $\hat{G}(z,z_0)$ are defined by (10).

For the application to kinked-curved crack growth similar to the one shown in Fig. 2, two dislocations symmetrically placed with respect to the center of the pre-existing crack must be considered. In this case we add to the right-hand side of (12) terms corresponding to the dislocation $-\alpha$ at point $-z_0$. This yields

$$p(x,z_0) = (\bar{\alpha}\bar{\beta} - \alpha\beta)\{[\hat{f}(x,z_0) - \hat{f}(x,-z_0)] + [\hat{f}(x,\bar{z}_0) - \hat{f}(x,-\bar{z}_0)]\}$$
$$+ (\bar{z}_0 - z_0)\{\alpha\bar{\beta}[\hat{g}(x,z_0) + \hat{g}(x,-z_0)] + \bar{\alpha}\beta[\hat{g}(x,\bar{z}_0) + \hat{g}(x,-\bar{z}_0)]\}. \qquad (14)$$

From the symmetry $C = 0$, and

$$\Phi_R'(z) = (\bar{\alpha}\bar{\beta} - \alpha\beta)[F(z,z_0) + F(z,\bar{z}_0)] + (\bar{z}_0 - z_0)[\alpha\bar{\beta}G(z,z_0) + \bar{\alpha}\beta G(z,\bar{z}_0)], \qquad (15)$$

where

$$F(z,z_0) = \left[1 - \frac{z}{z_0}\frac{X(z_0)}{X(z)}\right]\frac{z_0}{z^2 - z_0^2}$$

$$G(z,z_0) = \frac{\partial}{\partial z_0}F(z,z_0) = \left[1 - \frac{z}{z_0}\frac{X(z_0)}{X(z)}\right]\frac{2z_0^2}{(z^2 - z_0^2)^2} + \left[1 - \frac{zz_0}{X(z)X(z_0)}\right]\frac{1}{z^2 - z_0^2}; \qquad (16)$$

note that in equation $(8)_1$ of [2] and $(2.9)_1$ of [32], the term z/z_0 inside the brackets is missing, and that the corresponding equations $(8)_2$ and $(2.9)_2$ must be corrected accordingly.

3. Far-Field Stresses

Let the applied far-field stresses be denoted by $\sigma_{x\infty}$, $\sigma_{y\infty}$, and $\tau_{xy\infty}$, and observe that for a uniform body (no crack), the corresponding potentials are

$$\Phi'_{\infty 0} = (\sigma_{y\infty} + \sigma_{x\infty})/4, \qquad \Psi'_{\infty 0} = (\sigma_{y\infty} - \sigma_{x\infty})/2 + i\tau_{xy\infty}. \qquad (17)$$

For the open crack, $\Phi_{\infty R}$ and $\Psi_{\infty R}$ are required in order to remove the tractions $(\sigma_{y\infty} - i\tau_{xy\infty})$ on the pre-existing crack. Hence, direct calculation from (7) yields

$$\Phi'_{\infty R}(z) = \frac{1}{2}(\sigma_{y\infty} - i\tau_{xy\infty})\left[-1 + \frac{z}{X(z)}\right] \quad \text{for open pre-existing crack.} \qquad (18)$$

For a closed frictional crack, on the other hand, it is required that $\Phi_{\infty R}$ and $\Psi_{\infty R}$ lead to $\tau_{xy\infty} + \tau_{\infty R} = -\tau_c + \mu\sigma_{y\infty}$, $\sigma_{\infty R} = 0$, on the pre-existing crack. Hence, again from (7),

$$\Phi'_{\infty R}(z) = \frac{i}{2}(\tau_{xy\infty} - \mu\sigma_{y\infty} + \tau_c)\left[1 - \frac{z}{X(z)}\right] \quad \text{for closed frictional crack.} \qquad (19)$$

Note that the corresponding $\psi'_{\infty R}$ is obtained by substitution from (18) and (19) into $(9)_2$.

4. Singular Integral Equation

Let the crack extension profile be given by

$$x = c + g(r), \qquad y = f(r), \qquad (20)$$

where r measures length along the curved crack; see Fig. 6. Then

$$\theta(r) = \tan^{-1}(f'/g'). \qquad (21)$$

Denote by $\sigma_{\theta\theta}$ and $\tau_{r\theta}$ the hoop and shear stresses, and require that

$$\sigma_{\theta\theta} + i\,\tau_{r\theta} = 0 \quad \text{on the curved crack extension.} \qquad (22)$$

On the other hand,

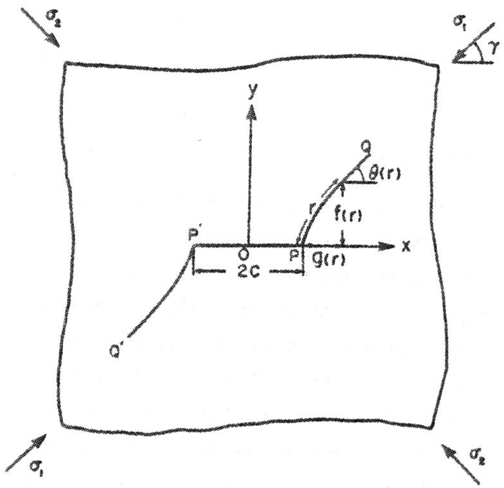

Figure 6

$$\sigma_{\theta\theta} + i\sigma_{r\theta} = \Phi' + \overline{\Phi'} + e^{i2\theta(s)}(\bar{z}\Phi'' + \Psi'), \qquad (23)$$

where the overall complex potentials are

$$\Phi = \Phi_D + \Phi_\infty, \qquad \Phi_D = \Phi_0 + \Phi_R,$$

$$\Phi_\infty = \Phi_{\infty 0} + \Phi_{\infty R}, \qquad (24)$$

with similar expressions for Ψ.

Consider now distributed dislocations of *density* $\alpha(r)$ on the crack extension path, where b in (2) is defined by

$$b = \frac{\partial}{\partial r}\{[u_r] + i[u_\theta]\}dr. \qquad (25)$$

Stress-free condition (22) and Eqs. (23) and (24) yield

$$\int_0^\ell [\Phi'_D + \overline{\Phi'_D} + e^{i\theta(s)}(\bar{z}\Phi''_D + \Psi'_D)]dr + \Phi'_\infty + \overline{\Phi'_\infty} + e^{i\theta(s)}(\bar{z}\Phi''_\infty + \Psi'_\infty) = 0, \qquad (26)$$

where ℓ is the length of the extended part of the crack. With $z_0 = c + g(r) + if(r)$ and $z = c + g(s) + if(s)$, Eq. (26) becomes

$$\int_0^\ell \frac{L_1(r,s;\alpha(r))}{s - r}dr + \int_0^\ell L_2(r,s;\alpha(r))dr + \sigma_{\theta\infty}(s) + i\tau_{r\theta\infty}(s) = 0, \qquad (27)$$

where

$$L_1(r,s;\alpha(r)) = \alpha(r)\left[\frac{1}{h(r,s)} - e^{i2\theta(s)}\frac{\overline{h(r,s)}}{(h(r,s))^2}\right] + \bar{\alpha}(r)\left[\frac{1}{\overline{h(r,s)}} + e^{i2\theta(s)}\frac{1}{h(r,s)}\right],$$

$$h(r,s) = \begin{cases} [g(s) - g(r) + i(f(s) - f(r))]/(s - r), & (s \neq r), \\ g'(s) + if'(s) & (s = r), \end{cases}$$

$$L_2(r,s;\alpha(r)) = -\frac{\alpha(r)}{z(s) + z_0(r)} - \frac{\bar{\alpha}(r)}{\bar{z}(s) + \bar{z}_0(r)} + e^{2i\theta(s)}\left[\frac{\alpha(r)(\bar{z}(s) + \bar{z}_0(r))}{(z(s) + z_0(r))^2} - \frac{\bar{\alpha}(r)}{z(s) + z_0(r)}\right] + \Phi'_R + \overline{\Phi'_R} + e^{i2\theta(s)}[(\bar{z}(s) - z(s))\Phi''_R + \bar{\Phi}'_R - \Phi'_R],$$

and

$$\sigma_{\theta\infty}(s) + i\tau_{r\theta\infty}(s) = \Phi'_\infty + \overline{\Phi'_\infty} + e^{i2\theta(s)}(\bar{z}\Phi''_\infty + \Psi'_\infty). \qquad (28)$$

The stress intensity factors at the extended crack tip are given by

$$K_I + iK_{II} = \lim_{r \to \ell^-} \{\tfrac{1}{2}(2\pi)^{3/2}(\ell - r)^{1/2} L_1(\ell, \ell; \alpha(\ell))\}. \quad (29)$$

FRACTURE CRITERIA

To calculate the branched-curved extension path of a pre-existing crack, a fracture criterion is needed. There are several criteria of this kind in the literature, which include: (1) the maximum hoop stress criterion [33]; the maximum strain energy density criterion [34]; the criterion of local symmetry [10,12]; and the criterion of maximum energy release rate which relates to Griffith's original ideas [35,36]. Except for the last one, all these criteria are "local" ones. In [24] I have discussed the relation between the second law of thermodynamics in the sense of Gibbs and a more "global" fracture criterion which has a strong bearing on the last above criterion. The condition of local symmetry, however, is quite easy to apply, and in most cases leads to results which are in close agreement with the maximum energy release rate criterion. Here, as in [2], this criterion will be used.

RESULTS AND DISCUSSION

It can be shown that in most cases the maximum of K_I occurs when K_{II} is almost zero. Hence the criterion of local symmetry is essentially the same as the criterion of maximum K_I. For the numerical calculation, we follow [2,32] and solve (27) incrementally, i.e., we find the orientation of an incremental straight growth such that K_I is maximized. Then we fix the incremental length such that $K_I = K_c$ is satisfied.

Calculations show [2,32] that for uniaxial compression similar to the one shown in Fig. 2, the crack extension begins at an initial angle of about 70° relative to the direction of the pre-existing crack, and then curves and becomes parallel with the axial load. An interesting result is that, if some lateral tension also exists, then after a critical length is attained the growth process becomes unstable, i.e. the crack extends spontaneously in the direction of the maximum compressive stress without an increase in the axial load. Figure 7 illustrates this. [In this figure, σ_1 is the minimum principal axial stress, and σ_2 is the maximum principal stress.] This important result can be used to explain axial splitting of brittle solids, the phenomenon of sheet fracture or exfoliation which

refers to cracks running parallel to the free surface in rock masses, rockburst in deep mines due to coupled crack growth and buckling of rock slabs, and surface spalling, all under far-field compressive loads; see Nemat-Nasser and Horii [2] for illustrations and more discussion.

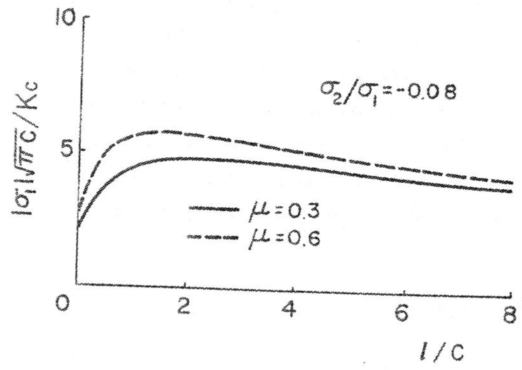

Figure 7

PERTURBATION RESULTS

For small deviations from straightness, crack extension paths may be estimated using a perturbation scheme; see [10,20,22,23,28]. As pointed out by this writer [23], the square-root singularity of the strain field near the tip of the pre-existing crack prior to crack extension requires that the crack extension path be defined by, Fig. 8,

$$Y = \omega X + \eta X^{3/2} + \gamma X^2 + \cdots, \quad (30)$$

where ω, η, γ,... are to be calculated. With this crack path, and with ℓ very small relative to 2c, one may express the stress potentials, Φ and Ψ, in Eq. (23) in terms of a set of stress potentials, F_j and W_j, $j = 0,1,\ldots$,

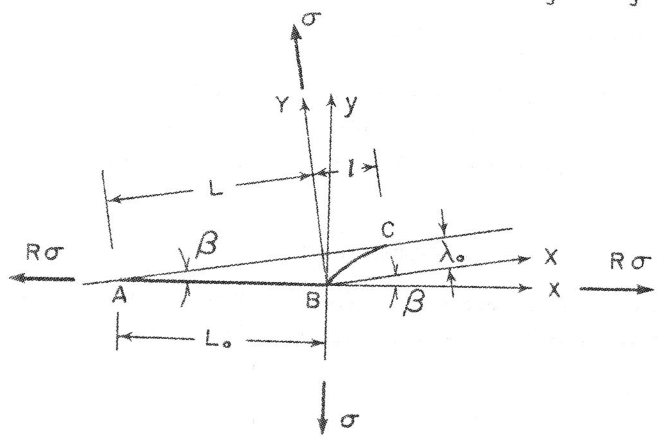

Figure 8

whose common cut in the Z-plane, $Z = X + iY$, is along the straight line AC, Fig. 8, and which are of the order of λ_0^j, where λ_0 is very small compared with the extended crack length, ℓ. The integral equation (26) may then be reduced to a sequence of integral equations for the stress functions F_j and W_j, and these equations can be solved consecutively, leading to explicit expressions for K_I and K_{II} at the tip of the extended crack, where the crack path extension is given by (30). With $\omega = \alpha - \beta$, and β defined in Fig. 8, one obtains [22]:

$$\alpha = -2\, k_2/k_1, \qquad \eta = \frac{8}{3}\left(\frac{2}{\pi}\right)^{\frac{1}{2}} \alpha \frac{T}{k_1},$$

$$\gamma = \alpha\left[4\,\frac{T^2}{k_1^2} + \frac{1}{2k_1}\frac{\partial k_1}{\partial L_0}\right] - \frac{1}{k_1}\frac{\partial k_2}{\partial L_0}, \tag{31}$$

where $L_0 = 2c$ is the initial crack length; T is the in-plane far-field stress difference, acting parallel to the pre-existing crack, i.e., $T = (R - 1)\sigma$ in Fig. 8, and k_1 and k_2 are the stress intensity factors for Modes I and II at the tip of the pre-existing crack *before* crack extension.

From (30) and (31) it is seen that when $k_2 \neq 0$, then there is an initial kink, followed by a smooth curve. In Fig. 1, the pre-existing crack A_2B_2 is *not* at a right angle with the edge AA_2. This introduces a non-zero k_2 at B_2. Hence, crack extension in this case involves an initial kink.

When $T = 0$ and $k_2 = 0$, Eqs. (31) show that $\alpha = 0$ and $\eta = 0$, but not necessarily γ. In this case, when $\partial k_2/\partial L_0 \neq 0$, smooth crack curving with profile

$$Y = -\beta X - \left\{\frac{1}{k_1}\frac{\partial k_2}{\partial L_0}\right\} X^2 + O(X^{5/2}) \tag{32}$$

is possible. In Fig. 1, the pre-existing crack AB is normal to the edge AA_2. This produces, for very small initial crack length, $k_2 \simeq 0$. However, $\partial k_2/\partial L_0 \neq 0$, and hence smooth crack curving occurs at almost zero initial kink angle.

ACKNOWLEDGMENT

This work has been supported by the Army Research Office under contract DAAG29-82-K-0147 to Northwestern University.

REFERENCES

[1] Karihaloo, B. L. and Nemat-Nasser, S., Thermally Induced Crack Curving in Brittle Solids, Analytical and Experimental Fracture Mechanics, G. C. Sih and M. Mirabile (eds.), Sijthoff & Noordhoff, 265 (1981).

[2] Nemat-Nasser, S. and Horii, H., Compression Induced Crack Kinking and Curving with Application to Splitting, Exfoliation, and Rockburst, EREL Tech. Report No. 81-11-44, Dept. of Civil Engrg., Northwestern University, Evanston, IL (1981); Compression-Induced Nonplanar Crack Extension with Application to Splitting, Exfoliation, and Rockburst, J. Geophys. Res., 87 (1982) 6805.

[3] Brace, W. F. and Bombolakis, E. G., A Note on Brittle Crack Growth in Compression, J. Geophys. Res., 68 (1963) 3709.

[4] Bieniawski, Z. T., Mechanism of Brittle Fracture of Rock, Part I--Theory of the Fracture Process, Int. J. Rock Mech. Min. Sci., 4 (1967) 395; Mechanism of Brittle Fracture of Rock, Part II--Experimental Studies, Int. J. Rock Mech. Min. Sci., 4 (1967) 407.

[5] Hoek, E. and Bieniawski, Z. T., Brittle Fracture Propagation in Rock Under Compression, Int. J. Fract. Mech., 1 (1965) 137.

[6] Fairhurst, C. and Cook, N. G. W., The Phenomenon of Rock Splitting Parallel to the Direction of Maximum Compression in the Neighborhood of a Surface, Proc. First Congr. Int. Soc. Rock Mech., 1, 687 (1966).

[7] Ingraffea, A. R., Mixed-Mode Fracture Initiation in Indiana Limestone and Westerly Granite, Proc. Symp. Rock Mech, 22, 186 (1981).

[8] Holzhausen, G. R., Sheet Structure in Rock and Some Related Problems in Rock Mechanics, Ph.D. Thesis, Stanford University, Stanford, CA (1978).

[9] Andersson, H., Stress Intensity Factors at the Tips of a Star-Shaped Contour in an Infinite Tensile Sheet, J. Mech. Phys. Solids, 17 (1969) 405; Erratum, J. Mech. Phys. Solids, 18 (1970) 437.

[10] Banichuk, N. V., Determination of the Form of a Curvilinear Crack by Small Parameter Technique (in Russian), Izv. Akad. Nauk SSSR Mekh. Tverd. Tela, 7 (1970) 130.

[11] Hussain, M. A., Pu, S. L., and Underwood, J., Strain Energy Release Rate for a Crack Under Combined Mode I and Mode II, ASTM Spec. Tech. Publ., 560, 55 (1974).

[12] Goldstein, R. V. and Salganik, R. L., Brittle Fracture of Solids with Arbitrary Cracks, Int. J. Fracture, 10 (1974) 507.

[13] Bilby, B. A., Cardew, G. E., and Howard, I. C., Stress Intensity Factors at the Tips of Kinked and Forked Cracks, Fracture 1977, 3, D. M. R. Taplin (ed.), U. of Waterloo Press, 197 (1977).

[14] Kitagawa, H. and Yuuki, R., Analysis of Branched Cracks Under Biaxial Stresses, Fracture 1977, 3, D. M. R. Taplin (ed.), U. of Waterloo Press, 201 (1977).

[15] Palaniswamy, K. and Knauss, W. G., On the Problem of Crack Extension in Brittle Solids Under General Loading, Mechanics Today, 4, S. Nemat-Nasser (ed.), Pergamon Press, 87 (1978).

[16] Wu, C. H., Elasticity Problems of a Slender Z-Crack, J. Elasticity, 8 (1978) 183.

[17] Wu, C. H., Maximum-Energy-Release-Rate Criterion Applied to a Tension-Compression Specimen with Crack, J. Elasticity, 8 (1978) 235.

[18] Wu, C. H., Fracture Under Combined Loads by Maximum-Energy-Release-Rate Criterion, J. Appl. Mech., 45 (1978) 553.

[19] Lo, K. K., Analysis of Branched Cracks, J. Appl. Mech., 45 (1978) 797.

[20] Cotterell, B. and Rice, J. R., Slightly Curved or Kinked Cracks, Int. J. Fracture, 16 (1980) 155.

[21] Karihaloo, B. L., Keer, L. M., and Nemat-Nasser, S., Crack Kinking Under Nonsymmetric Loading, EREL Tech. Report No. 79-5-15, Dept. of Civil Engrg., Northwestern University, Evanston, IL (1979); Eng. Fract. Mech., 13 (1980) 879.

[22] Karihaloo, B. L., Keer, L. M., Nemat-Nasser, S., and Oranratnachai, A., Approximate Description of Crack Kinking and Curving, EREL Tech. Report No. 79-5-17, Dept. of Civil Engrg., Northwestern University, Evanston, IL (1979); J. Appl. Mech., 48 (1981) 515.

[23] Nemat-Nasser, S., On Stability of the Growth of Interacting Cracks, and Crack Kinking and Curving in Brittle Solids, EREL Tech. Report No. 80-5-31, Dept. of Civil Engrg., Northwestern University, Evanston, IL (1980); Numerical Methods in Fracture Mechanics, Proc. Second Int. Conf., D. R. J. Owen and A. R. Luxmoore (eds.), Pineridge Press, 687 (1980).

[24] Nemat-Nasser, S., The Second Law of Thermodynamics and Noncollinear Crack Growth, Proc. Third Engineering Mechanics Div. Spec. Conf., ASCE, 449 (1979).

[25] Hayashi, K. and Nemat-Nasser, S., Energy Release Rate and Crack Kinking, EREL Tech. Report No. 80-1-23, Dept. of Civil Engrg., Northwestern University, Evanston, IL (1980); Int. J. Solids Struct., 17 (1981) 107.

[26] Hayashi, K. and Nemat-Nasser, S., Energy Release Rate and Crack Kinking Under Combined Loading, EREL Tech. Report No. 80-6-33, Dept. of Civil Engrg., Northwestern University, Evanston, IL (1980); J. Appl. Mech., 48 (1981) 520.

[27] Hayashi, K., and Nemat-Nasser, S., On Branched, Interface Cracks, EREL Tech. Report No. 80-6-34, Dept. of Civil Engrg., Northwestern University, Evanston, IL (1980); J. Appl. Mech., 48 (1981) 529.

[28] Karihaloo, B. L., On Crack Kinking and Curving, Mechanics of Materials, 1 (1982) 189.

[29] Muskhelishvili, N. I., Some Basic Problems in the Mathematical Theory of Elasticity, Noordhoff (1953).

[30] Erdogan, F., On the Stress Distributions in Plates with Collinear Cuts Under Arbitrary Loads, Proc. Fourth U. S. Nat. Congress of Appl. Mech., 1, 547 (1962).

[31] Rice, J. R., Mathematical Analysis in the Mechanics of Fracture, Fracture, 2, H. Liebowitz (ed.), Academic Press, Chapter 3 (1968).

[32] Horii, H. and Nemat-Nasser, S., Curved Crack Growth in Brittle Solids Under Far-Field Compression, 1982 Advances in Aerospace Structures and Materials, R. M. Laurenson and U. Yuceoglu (eds.), AD-03, ASME, 75 (1982).

[33] Erdogan, F. and Sih, G. C., On the Crack Extension in Plates Under Plane Loading and Transverse Shear, J. Basic Engrg., 85 (1963) 519.

[34] Sih, G. C., Introductory Chapter: A Special Theory of Crack Propagation, Mechanics of Fracture, 1, Noordhoff (1972).

[35] Griffith, A. A., The Phenomena of Rupture and Flow in Solids, Phil. Trans. R. Soc., A221 (1921) 163.

[36] Griffith, A. A., The Theory of Rupture, Proc. First Int. Congress of Appl. Mech., 55 (1924).